United States Environmental Protection Agency

Screening Methods for Metal-Containing Nanoparticles in Water

APM 32

RESEARCH AND DEVELOPMENT

EPA/600/R-11/096
September 2011
www.epa.gov

Screening Methods for Metal-Containing Nanoparticles in Water

APM 32

Prepared by

Edward M. Heithmar
U.S. Environmental Protection Agency
National Exposure Research Laboratory
Environmental Sciences Division
Environmental Chemistry Branch
Las Vegas, NV 89119

U.S. Environmental Protection Agency
Office of Research and Development
Washington, DC 20460

Abstract

Screening-level analysis of water for metal-containing nanoparticles is achieved with single particle-inductively coupled plasma mass spectrometry (SP-ICPMS). This method measures both the concentration of nanoparticles containing an analyte metal and the mass of the metal in each particle. SP-ICPMS is capable of sample throughputs of over twenty samples per hour. In this report, the screening capability of SP-ICPMS is demonstrated in a study of transformations of silver nanoparticles in surface water. Test water samples were collected from two fresh water sites and two estuary sites. The effects of salinity, particle concentration, particle size, and particle surface chemistry on relative rates of transformations were studied. At high silver particle concentration ($2.5x10^7$ mL^{-1}) shifts in the particle silver mass distribution measured by SP-ICPMS indicated increased aggregation rate at high salinity, as reported by others. However, at low silver particle concentration ($2.5x10^5$ mL^{-1}), which is closer to expected environmental concentrations, aggregation was minimal even in highly saline estuary water. At the low concentration, a much more pronounced increase in either dissolved silver or silver-containing nanoparticles too small to be distinguished from dissolved silver was observed. These data were operationally defined in this report as "dissolved" silver. Comparison of transformations of 50-nm and 100-nm silver indicated that rates of both aggregation and apparent dissolution are higher for the smaller particles at the same particle concentration. Transformations for citrate-capped and polyvinylpyrrolodone-capped silver nanoparticles were similar.

Notice

The United States Environmental Protection Agency's Office of Research and Development partially performed and funded the research described here. Mention of trade names or commercial products does not constitute endorsement or recommendation for use.

Contents

List of Figures

List of Tables

Abbreviations and symbols

AFM	Atomic force microscopy
APHA	American Public Health Association
c_a	Analyte concentration in aqueous sample (g/mL)
c_p	Particle concentration in aqueous sample (mL^{-1})
DI	Deionized
DLS	Dynamic light scattering
EDS	Energy-dispersive X-ray spectrometry
ε_n	Nebulization transport efficiency (dimensionless)
ENM	Engineered nanomaterials
EPA	Environmental Protection Agency
FFF	Field flow fractionation
Flow-FFF	Flow field flow fractionation
HDC	Hydrodynamic chromatography
ICON	International Council on Nanotechnology
ICPMS	Inductively coupled plasma mass spectrometry
IRZ	Initial radiation zone
LDPE	Low-density polyethylene
$m_{a,p}$	Analyte element mass in the particle (g)
$n_{i,p}$	Number of analyte ions detected (demensionless)
NOM	Natural organic matter
NTA	Nanoparticle tracking analysis
PDI	Polydispersity index (dimensionless)
PSU	Practical salinity units (dimensionless)
PVP	Polyvinylpyrrolodone
$q_{i,a}$	Ionized analyte flux (s^{-1})
q_p	Particle flux (s^{-1})
q_s	Sample uptake rate ($mL\ s^{-1}$)
r_g	Radius of gyration
r_h	Hydrodynamic radius
RSD	Relative standard deviation
Sed-FFF	Sedimentation field flow fractionation
SEM	Scanning electron microscopy
SLS	Static light scattering
SP-ICPMS	Single particle - inductively coupled plasma mass spectrometry
TEM	Transmission electron microscopy
WDS	Wavelength-dispersive X-ray spectrometry
ζ	Zeta (potential; usually mv)

Acknowlegements

I thank Tara Schraga of the U.S. Geological Survey and David Carpenter of the Southwest Florida Water Management District for collecting the water samples, and Jay Kuhn of Analytical Resources, Inc. for access to the PerkinElmer NexION ICPMS. Chady Stephan of PerkinElmer conducted some of the experiments with me and participated in valuable discussions regarding the data. Emily Siska, a student contractor for the Environmental Protection Agency, provided much needed laboratory support.

Background

Engineered nanomaterials (ENMs) are increasingly being incorporated in industrial, consumer, medical, and agricultural products. This is because ENMs exhibit unique optical, electrical, and chemical properties that can impart beneficial characteristics to the product into which they are incorporated. However, these unique properties also affect the environmental behavior of ENMs. Their transport, fate, exposure potential, and effects are not predicted by those of either the corresponding bulk materials or dissolved chemicals.

Most ENMs currently in production can be categorized as either metal-containing ENMs (i.e., metals, metal oxides, or semiconducting quantum dots) or carbon-based (i.e., fullerenes and their derivatives, and carbon nanotubes). ENMs containing metals have a greater potential to enter the environment than carbon-based ENMs. This is a result of the fact that the major uses of metal-containing ENMs are in dispersive applications, while carbon-based ENMs are generally incorporated into solid composites. This increased exposure potential for metal-containing ENMs has motivated intense research into their environmental processes, such as transformation, transport and fate, exposure pathways, and potential adverse effects on humans and sensitive organisms.

Detection, quantification, and characterization of ENMs, including measurement of nanoparticle concentration and characterization of particle size distribution, are critical to all aspects of this exposure research. Nanoparticle concentration and size distribution largely control how they behave in the environment. Highly selective detection, quantification, and characterization methods are important for many types of nanomaterials environmental research; less selective methods that can rapidly screen samples for metal-containing nanoparticles are also needed.

This report focuses on the application of a new method, single-particle-inductively coupled plasma mass spectrometry (SP-ICPMS), for rapid screening-level measurement of nanoparticle dispersions. The method is being developed at the Environmental Sciences Division of EPA's National Exposure Research Laboratory. SP-ICPMS has demonstrated promise as a practical analytical method for characterization of metal-containing ENMs in environmental waters. This report will: (1) briefly review of the role of characterization of metal-containing ENMs in the exposure research of these novel materials; (2) discuss methods currently available for the measurement of various ENM exposure metrics; and (3) describe the limitations of existing methods for studying ENMs in real environmental systems. A brief review of the theory of SP-ICPMS will also be provided. A study that applies SP-ICPMS in a stand-alone screening-level mode will be described in detail. Specifically, SP-ICPMS will be used to study transformations of silver nanoparticles in surface water.

Rationale for research on metrology methods for metal-containing ENMs

A workshop on the eco-responsible design and development of ENMs was conducted by the International Council on Nanotechnology (ICON) in 2009 (Alvarez, Colvin et al. 2009). Fourteen key research priorities that would inform designing, using and disposing of ENMs to enhance responsible development of these materials were identified by the approximately 50 researchers invited to the workshop. The fourteen priorities were then ranked against two criteria. First, the relative importance of the research in understanding how to design and develop ENMs in an eco-responsible manner was assessed. Second, the current gap in the state-of-knowledge for each research priority was ranked. The workshop also assessed the amount of effort required to sufficiently satisfy the science gap posed by each research priority. The results of these three assessments are summarized here (Table 1).

Table 1. Ranking (in descending order) of 14 key research priorities for eco-responsible ENM design (adapted from Alvarez, Colvin et al. 2009).

Importance for eco-responsible design	Gap in state-of-knowledge	Effort needed
Metrology, analytical methods	Metrology, analytical methods	High
Predictive models of release	Structure-activity relations	High
Structure-activity relations	Boavailability and bioaccumulation	Medium-high
Dose-response (sub-lethal)	Sources/environmental fluxes	Medium
Boavailability and bioaccumulation	Trophic transfer	Medium
Identify relevant sentinel organisms	Uptake mechanisms	Low
Trophic transfer	Intra-organism distribution	Low
Industrial ecology/green chemistry	Industrial ecology/green chemistry	Medium
Sources/environmental fluxes	Impact on environmental infrastructure	Medium
Impact on environmental infrastructure	Predictive models of release	High
Uptake mechanisms	Assessing regulatory framework	Medium
Assessing regulatory framework	Dose-response (sub-lethal)	Medium-high
Intra-organism distribution	Waste minimization/recycling	Medium
Waste minimization/recycling	Identify relevant sentinel organisms	Low

Metrology to detect, quantify, and characterize ENMs ranked highest in importance for enabling eco-responsible design of ENMs. This area also ranked as least developed in terms of state-of-knowledge. Consequently, the workshop recommended a great deal of effort be applied in metrology to detect, quantify, and characterize ENMs.

The workshop's emphasis on the need for research on detection, quantification, and characterization of ENMs stems from a number of factors. First, these metrology tools are vital for the success of virtually every area of research on the environmental behavior, exposure potential, and possible adverse effects of ENMs. Monitoring environmental occurrence and distribution of ENMs, as well as determining temporal trends in these data, requires metrology methods. Process research into ENM transformation, transport, and fate requires methods to measure and characterize ENMs in each compartment of a laboratory system. Toxicity research requires quantifying and characterizing the ENMs in the original dosing material, and possible changes in concentration and size distribution induced by the test system must also be measured.

Often, toxicity testing requires measuring internal ENM dose in the test organisms. Finally, emerging exposure models for ENMs (Mueller and Nowack 2008) require quantification of ENM releases and ENM measurements in the environment for model validation.

The low level of the state-of knowledge for detection, quantification, and characterization of ENMs is based in part on the complex set of metrics that need to be measured. Compound concentration is often the only relevant metric for conventional pollutants in evaluating exposure potential, because these are released and transported in dissolved form. Conversely, for ENMs, in addition to mass concentration, measurement of particle concentration and particle size distribution is usually required, because the environmental stability and mobility of ENMs are influenced by their particle size. There are also several ways of measuring particle size that may be important depending on the application, including particle mass, volume, and hydrodynamic diameter [the theoretical diameter of an equivalent spherical particle and its electric double layer (Hassellöv, Readman et al. 2008). In addition to mass concentration, particle concentration, and size distribution, other metrics sometimes affect environmental behavior of ENMs. Surface area affects reaction rates of ENMs; therefore, their catalytic activity, and surface area can also mediate ENM toxicity (Schulte, Geraci et al. 2008). Surface charge or zeta potential (ζ) affects the inter-particle repulsive forces of ENM suspensions, which influences their tendency to aggregate (Kim, Lee et al. 2008). ENM aspect ratio, the ratio of the longest to the shortest dimension of the nanoparticles, sometimes influences toxicity of long and narrow ENMs such as carbon nanotubes (Takagi, Hirose et al. 2008). Therefore, in nearly all research efforts related to the environmental behavior, exposure potential, and possible adverse effects of ENMs, methods are required for quantifying mass and particle concentration, and at least one metric related to size distribution. Other metrics such as surface area, surface charge, and particle shape may also be required, depending on the environmental behavior or effect being studied.

There is a paucity of practical methods for detecting, quantifying, and characterizing nanomaterials in complex media. For ENMs in pure suspensions, there are several methods available to quantify mass and particle concentrations, as well as characterize size distributions. For example, characterizing ENM starting materials used in laboratory studies is often relatively straightforward. However, the test systems in which the starting materials are studied often alter these metrics, and there are few methods for measuring them in these more complex systems (Alvarez, Colvin et al. 2009). Natural environmental samples are usually even more analytically challenging than laboratory test systems, and no practical methods have yet been published for detecting, quantifying, and characterizing ENMs in environmental media (Handy, von der Kammer et al. 2008). Several common properties of natural environmental media contribute to the dearth of applicable ENM metrology tools for these sample types. Natural systems generally have very low concentrations of ENM particles (Kiser, Westerhoff et al. 2009), so the sensitivity of many analytical techniques is insufficient. In addition, natural colloids containing the analyte element used to detect the ENM are often present (Klaine, Alvarez et al. 2008). In the case of metal-containing ENMs, most analytical techniques measure total element concentration, and many natural colloids include minerals that contain a wide range of metals, so background interference is an issue. Finally, particle size determination can be confounded by dissolved metals adsorbed to relatively large natural organic matter (NOM) particles.

Methods for a wide range of characterization metrics might be developed for simple systems such as laboratory media; however, it is unlikely that methods for many ENM characteristics, such as surface charge and aspect ratio, can be developed for natural systems. However, methods must be developed that can at least selectively detect, and quantify ENM particle concentration, as well as characterize the size distributions of metal-containing ENMs, in natural environmental media. In addition, screening-level methods must be developed that will allow rapid analysis of samples for potential ENM content. These screening techniques will be required because selective techniques will likely involve time-consuming separations, and therefore will not be applicable to large numbers of samples. In addition, rapid screening-level techniques could be used to study environmental processes, such as aggregation and dissolution, that occur on time scales too rapid for separation-based techniques.

Current methods for detecting, quantifying, and characterizing ENMs

Imaging techniques are currently the most common methods for characterizing the size and shape of ENMs (Lin and Yang 2005; Pyrz and Buttrey 2008). Either scanning electron microscopy (SEM) or transmission electron microscopy (TEM) can be employed. In some studies, atomic force microscopy (AFM) can also be used (Ebenstein, Nahum et al. 2002). In some cases, AFM can provide additional information such as adsorption forces. SEM or TEM coupled with X-ray spectrometry, in either the energy-dispersive (EDS) or wavelength-dispersive (WDS) modes, can definitively identify metal-containing nanoparticles. However, particle concentrations must be high (generally $>10^9$ mL^{-1}) to reliably find nanoparticles using any of the imaging methods. Also, the lack of representative sampling techniques for imaging methods precludes quantification of particle concentration. Current sampling methods can also produce changes in the size distribution of the ENM (Tang, Wu et al. 2009). Finally, imaging techniques are generally not practical for environmental characterization in natural media because of background colloids. In environmental media, metal-containing ENMs cannot be distinguished from colloid particles containing the same metal (Tiede, Hassellöv et al. 2009).

Representative nanoparticle size distributions can be obtained by a variety of light scattering methods, because they rely on measuring a signal that is produced by the collection of all ENM particles in a large volume of sample, in contrast to the minute volume sampled by the imaging methods. ENM size distribution by light scattering methods is also possible at lower concentrations (ca. 10^6-10^7 mL^{-1}) than allowed by imaging techniques. Dynamic light scattering (DLS) is the most prevalent light scattering characterization tool. It uses the autocorrelation function of scattered laser light to calculate the hydrodynamic radius (r_h) distribution (Filella, Zhang et al. 1997). DLS can also measure ζ potential when performed on a sample in an oscillating electric field. A second light scattering method, static light scattering (SLS), also known as multi-angle light scattering, measures the radius of gyration (r_g) (Kammer, Baborowski et al. 2005). It has been demonstrated that the ratio r_g/r_h can provide information on ENM aspect ratio (Schurtenberger, Newmen et al. 1993). DLS and SLS are most applicable for ENM suspensions with narrow size distributions. Light scattering intensity is related to particle diameter in a non-linear fashion, and in more polydisperse samples, scattering by large particles distorts the calculation of the size distribution. In contrast to DLS and SLS, nanoparticle

tracking analysis (NTA) measures the scatter from individual particles. Therefore, NTA can accurately determine size distributions in polydisperse suspensions. None of the light scattering techniques are element selective. They measure the size distribution of all nanoparticles regardless of composition. Therefore, light scattering methods are not applicable in complex natural media.

To detect, quantify, and characterize metal-containing ENMs in natural media, an element-selective detection method is required to reduce interference from background natural colloids. Inductively coupled plasma mass spectrometry (ICPMS) is by far the most common such detection approach, because of its high sensitivity. However, most element-selective detection techniques, including ICPMS, cannot characterize particle size distribution. This has led to the increasing use of hyphenated analytical methods, where a size separation, usually by some form of chromatography, is coupled on-line to ICPMS. Recently, the most common size separation technique has been a form of field flow fractionation (FFF). FFF comprises several variants. In each, a laminar flow of an eluent (usually an aqueous surfactant solution) carries a plug of sample down a narrow channel. A force field is applied orthogonal to the laminar flow, forcing nanoparticles toward the channel wall. Size separation is effected by the balance between this force and the different diffusivities determined by particle sizes. Smaller particles diffuse higher, into a faster portion of the laminar-flow profile. Therefore, smaller particles elute before larger particles. The intensity vs. retention time profile produced by FFF is called a fractogram. A number of force fields can be used. The FFF technique most commonly used for size separation of ENMs is flow-FFF (Lesher, Ranville et al. 2009), where the orthogonal force is produced by a flow through a channel wall that is porous to eluent but not to nanoparticles. A gravity field has been used less often in a technique known as sedimentation-FFF (or sed-FFF). The two forms of FFF are complementary in that separations are produced by different particle properties – r_h in flow-FFF, and buoyant mass in sed-FFF. While sed-FFF affords higher size resolution, flow-FFF is easier to implement and is applicable to a wider range of ENM particle sizes: hence, the greater popularity of flow-FFF. Flow-FFF-ICPMS does have an experimental complication, in that nanoparticle interactions with the porous membrane wall can lead to peak tailing and even irreversible adsorption.

Another hyphenated analytical approach for ENM size characterization uses a separation technique known as hydrodynamic chromatography (HDC) (Tiede, Boxall et al. 2010). In HDC-ICPMS, the ENM particles pass through a column packed with a material such as silica in a eluent under laminar-flow conditions. Small nanoparticles can approach the particle surfaces closer than large particles, therefore experiencing a lower average flow velocity. The fractogram of HDC-ICPMS is inverted compared to that of FFF-ICPMS: small particles elute after larger particles in HDC-ICPMS. FFF-ICPMS offers higher resolution, while HDC-ICPMS often effects a more rapid separation.

Both flow-FFF-ICPMS and HDC-ICPMS provide elemental information in addition to size distribution. Either can be applied to moderately complex systems like laboratory test media. However, the application of either for natural environmental media is limited. Fractograms measure the total analyte metal concentration flowing to the ICPMS. Therefore, neither FFF-ICPMS nor HDC-ICPMS can determine the chemical state of the metal. For example, a 10 ng/mL concentration of silver detected at a retention time related to a given r_h

could be produced by 10 ng/mL silver ENM, but it could also result from approximately 130 ng/mL of AgCl nanoparticles having the same r_h. Furthermore, a high concentration of NOM with the same r_h could adsorb dissolved silver and produce a similar signal at the same retention time. Therefore, these hyphenated methods provide an upper-limit for the potential concentration of ENMs in natural media, but not a definitive determination of ENMs.

Single particle - inductively coupled plasma mass spectrometry

The limitations of hyphenated approaches to metal-containing ENM size characterization when applied to natural media have encouraged development of single particle - inductively coupled plasma (SP-ICPMS). This technique was introduced by Degueldre's group to characterize various colloids (Degueldre and Favarger 2004; Degueldre, Favarger et al. 2004), and later gold nanoparticles (Degueldre, Favarger et al. 2006). Recently, Ranville's group described a preliminary application of SP-ICPMS to characterize silver nanoparticles in municipal waste water (Monserud, Lesher et al. 2009), and Hassellöv coupled SP-ICPMS with flow-FFF (Hassellöv 2009).

The principle underlying SP-ICPMS is simple. Metal-containing nanoparticles entering an ICPMS plasma produce discrete ion plumes of the analyte metal isotopes over short time periods (e.g., < 1 ms). If the ICPMS signal is monitored with high temporal resolution (e.g., ≤10 ms per data point) background in each data point from dissolved analyte metal or plasma matrix ions (Lam and Horlick 1990) diminishes to a very low average ion count per data point. The ion plume pulses from the nanoparticles produce several ions in a single data point, making them easily distinguishable. The metal-containing nanoparticle concentration in the sample is obtained by measuring the frequency of the ion plume pulses. The analyte metal mass contained in each individual nanoparticle is independently calculated by the ion intensity of its corresponding ion plume.

The quantification metrics produced by SP-ICPMS are complementary to those produced by hyphenated analytical methods like FFF-ICPMS and HDC-ICPMS (Table 2). Either SP-ICPMS or a hyphenated method, used as stand-alone techniques, can only be a screening technique giving an upper bound for the concentration of metal-containing ENMs. Although SP-ICPMS measures the metal of interest in each particle, it provides no direct measurement of the particle diameter. Using the example of silver ENM again, detection of SP-ICPMS pulses of a given intensity could be caused by silver ENM nanoparticles of a certain diameter, or they could be produced by larger nanoparticles of insoluble silver salts, such as AgCl or AgS. Because of the complementary nature of the metrics produced by SP-ICPMS and hyphenated analytical methods, FFF-SP-ICPMS or HDC-SP-ICPMS could provide very selective detection, quantification, and size characterization in natural environmental media.

Table 2 Quantification and characterization metrics produced by SP-ICPMS and by hyphenated analytical methods.

SP-ICPMS	Hyphenated Analytical Methods
Measures the particle concentration of metal-based nanoparticles, as well as the mass of metal in each particle.	Measures total metal concentration as a function of nanoparticle size fraction.
Does not provide direct information on particle diameters.	Does not provide information on number or characteristics of metal-based particles.

Theory and Calibration Principles of SP-ICPMS

A complete understanding of the theory of SP-ICPMS requires consideration of some general processes that affect signal in all forms of ICPMS, including conventional ICPMS of analyte in solution. The processes are the same in conventional and single particle implementations of ICPMS. Partly because of these common processes, dissolved analyte measurements can be used in the calibration of particle element mass metric determined by SP-ICPMS.

In conventional ICPMS of an aqueous sample, an aerosol of droplets is produced by some form of nebulizer (Taylor 2001). Large aerosol droplets (> 5-10 μm in diameter) do not contribute to analyte signal and cause noise in the plasma; therefore, a spray chamber is usually employed to remove these large droplets by collisions with the chamber walls. This results in a fine aerosol entering the plasma, the droplet flux of which is typically greater than 10^6 s^{-1}. At ng/mL analyte concentrations, each droplet contains less than a few thousand analyte atoms. The efficiency of the total sampling process that results in analyte-containing aerosol in the plasma is termed the nebulization transport efficiency, ε_n. This quantity is usually between 2% and 30%, depending on specific sample introduction system and operating conditions. Aerosol is evaporated in the region within the ICP load coil known as the preheating zone of the plasma. The salts containing the analyte element vaporize in this region. Atomization occurs in the region from zero to several millimeters downstream from the load coil. This region is the initial radiation zone (IRZ) (Koirtyohann, Jones et al. 1980). Downstream from the IRZ is the normal analytical zone; ionization occurs in this region (Thomas 2004). In a typical ICP, vaporization, atomization, and ionization processes once aerosol is in the plasma are usually >80% efficient for most elements (O'Connor and Evans 1999). This is true for both conventional ICPMS and SP-ICPMS

ICPMS of nanoparticles differs from conventional ICPMS of dissolved analyte because of the way analyte is distributed within the aerosol. In conventional ICPMS, a each droplet contains a small number of analyte atoms. The large number of droplets results in a relatively

constant flux of ionized analyte; therefore, a fairly constant signal is produced. Typically, the sampling time per data point (called the dwell time) is set at ≥100 ms, to minimize signal variation due to counting statistics or noise in the sampling process. In the case of ICPMS of nanoparticles, the great majority of aerosol droplets contain no nanoparticles. If there is any dissolved analyte in the sample, it is distributed as in conventional ICPMS, and it contributes to a fairly constant background. Only a small fraction of droplets contain a nanoparticle at low ENM concentration, and generally only one nanoparticle is contained in a droplet. However, each nanoparticle can produce a plume of millions of ions that enter the mass spectrometer interface over a period of about 500 µs (Gray, Olesik et al. 2009; Heithmar 2009). The resulting signal is composed of the low constant background with periodic pulses of large numbers of analyte ions detected. In contrast to conventional ICPMS, SP-ICPMS is implemented with very short dwell times to improve the contrast between signal produced by dissolved analyte and the large, fast pulses from analyte in nanoparticles. For example, if the dwell time is set at 1 ms, a 1 pg/mL dissolved silver background would typically result in an average background signal of 0.1-0.5 ions in a single dwell period. By contrast, a 50 nm silver nanoparticle containing about 6.2×10^{-16} g silver (3.4×10^{6} atoms) would typically produce a signal of 20-50 ions in the same 1 ms dwell period (transmission efficiencies of quadropole mass filters are typically ca. 10^{-5}).

This theory of SP-ICPMS results in an easily calibrated signal if two assumptions are met. First, every nanoparticle that reaches the plasma must be detected as an ion plume. This requires a sufficiently long residence time, so the ion plume expands enough to substantially fill the cross section of the central channel of the plasma. If so, equation 1 is valid.

$$(1) \qquad q_p / c_p = q_s \, \varepsilon_n,$$

where q_p = flux of particles detected in plasma (s^{-1}), c_p = concentration of nanoparticles containing the detected metal in the sample (mL^{-1}), q_s = sample uptake rate (mL s^{-1}), and ε_n = nebulization efficiency (dimensionless). Note that q_s and ε_n are properties of the ICPMS instrument conditions and independent of the element. Therefore, equation 1 can be used to calculate their product using any type of nanoparticle suspension of known c_p.

The second assumption of quantitative SP-ICPMS calibration theory is that ICPMS sensitivity is constant for an analyte, irrespective of whether it is dissolved or contained in nanoparticles. Again, this requires that the residence time in the plasma to be sufficiently long. If so, equation 2 is valid.

$$(2) \qquad m_{a,p} = [q_s \, \varepsilon_n \, c_a / q_{i,a}] \, n_{i,p} = k \, n_{i,p},$$

where $m_{a,p}$ = mass of analyte element in a single nanoparticle (g), $n_{i,p}$ = number of ions of analyte element detected in the corresponding plume (number of ions detected in a single SP-ICPMS pulse), c_a = the analyte concentration in a dissolved standard of the analyte (g mL^{-1}), $q_{i,a}$ = ion flux measured for the dissolved standard (s^{-1}). For each analyte element, calibration of the element mass in individual particles (calculation of the response factor k) requires only the $q_s \, \varepsilon_n$ product from Equation 1 and analysis of a known concentration of dissolved analyte element using a conventional ICPMS standard).

Equation 2 provides calibration of nanoparticle element mass. The calibration of nanoparticle concentration is provided by rearrangement of equation 1 for any unknown nanoparticle suspension, once $q_s \varepsilon_n$ has been determined:

(3) $$c_p = q_p / q_s \varepsilon_n.$$

SP-ICPMS as a screening method for metal-containing nanoparticles in water

As a screening tool for metal-containing nanoparticles in natural media, stand-alone SP-ICPMS is potentially more useful than hyphenated methods of analysis. Analysis by SP-ICPMS can be applied to large numbers of samples, because it can achieve throughputs of over twenty samples per hour. By comparison, typical hyphenated analyses can take 20-40 minutes each. Also, SP-ICPMS has less potential for artifacts due to ENM adsorption. Finally, detection limits of ENMs by SP-ICPMS are potentially much lower than those that have been obtained by flow-FFF-ICPMS.

In addition to the ability to analyze large sample sets, the speed of screening-level SP-ICPMS also allows rapid transformations of metal-containing ENMs to be studied. The particle size distribution must not change significantly during the time required for size distribution analysis, which limits the hyphenated sizing methods to relatively slow transformations. In contrast, batch analysis by SP-ICPMS can be easily applied to studying size-distribution transformation processes with characteristic times of 2-3 minutes, and flow-injection experiments can be designed to study even faster processes.

This report will describe the application of SP-ICPMS as a stand-alone screening method to study time-resolved size-distribution transformations of silver ENM suspensions in natural surface waters. Size distribution is a critical parameter in predicting the mobility of nanoparticles, because larger particles fall out of the water column more quickly than small particles. The size distributions of ENMs are known to be affected by water chemistry, particularly by ionic strength (as determined in most surface waters by salinity) and NOM (French et al. 2009; Liu et al. 2010). In the study described in this report, the effects of water chemistry (particularly salinity), nanoparticle concentration, nanoparticle size, and nanoparticle surface chemistry on the size-distribution will be measured as a function of exposure time. Four surface waters of divergent water chemistry will be studied. Size distributions at exposure times of two to 3000 minutes will be measured. Transformation processes will be studied at both a high particle concentration typical of previously published studies (2.5×10^7 mL^{-1}) and a more environmentally relevant 2.5×10^5 mL^{-1}. Transformations of silver nanoparticle suspensions with mean diameters of 50 nm and 100 nm will be investigated. Finally, transformation of citrate and polyvinylpyrrolodone (PVP) capped silver nanoparticles will be compared.

Experimental

Standards and reagents

The purchased silver nanosphere standard suspensions were NanoXact^{TM} (Nanocomposix, San Diego, CA). The suspensions were quite monodisperse (RSD 8-10%) and the total silver concentration of each was 20 mg/L. The mean silver nanoparticle mass in femtograms and the suspension particle concentration were calculated from the mean nanoparticle diameter determined by the manufacturer by TEM (Table 3). Dilutions were made with laboratory deionized water.

Table 3. Size, mass, and particle-concentration metrics for silver nanosphere standards.

Nanoparticle (capping agent)	Mean Diameter (nm)	Diameter RSD (%)	Ag nanoparticle mass (fg)	Particle concentration (mL^{-1})
50 nm (citrate)	49.1	9.1	0.65	$3.1x10^{10}$
50 nm PVP	53.4	9.4	0.84	$2.3x10^{10}$
100 nm (citrate)	99.1	8.3	5.30	$3.7x10^{9}$

Water sampling sites

Sites for the silver transformation studies were selected with the intention of getting a range of salinities and NOM. One lake, one river, and two estuary sites were selected as water sources for the transformation study. The lake site was at Lake Hancock and the river site was on the Alafia River, both in west-central Florida (Figure 1). Lake Hancock is heavily impacted by agricultural runoff and its unfiltered sample was highly colored with algae. The Alafia River is typical of central Florida rivers, having high tannin content and a brown unfiltered sample color (Fgure 2).

The two estuary sampling sites were both located on the San Francisco Bay and are regular sampling locations (Stations 7 and 31) of the fresh water sampling site locations, with latitude and longitude.of the U.S. Geological Survey (USGS 2011). Station 7 is isolated from the mouth of the Bay by narrow straights, while Station 31 is in the wide lower arm of the Bay with direct access to the mouth of the Bay (Figure 3). Therefore, salinity at Station 7 is generally lower than at Station 31.

Figure 1. Fresh water sampling site locations, with latitude and longitude.

Figure 2. Water samples as received from the sampling sites before filtration. From left to right: San Francisco Bay Station 7, San Francisco Bay Station 31, Lake Hancock, and Alafia River. Note the color of the freshwater sites caused by algae (Lake Hancock) or tannin (Alafia River).

Figure 3. Estuary water sampling site locations, with latitude and longitude.

Water sampling, sample handling, and storage

The fresh water samples were collected on April 10, 2010. They were collected as a single grab sample by opening an empty 1-L low-density polyethylene (LDPE) bottle approximately 0.3 m below the surface of the water and capping the completely filled bottle before bringing it to the surface. The estuary samples were collected at a depth of 1 m via the sampling pump on the USGS research ship and collected in 1-L LDPE bottles. Salinities were measured on-board with a salinity meter in practical salinity units (PSU).

Water samples were maintained at ca. 4 °C until analysis. Samples were filtered through a 20 μm polypropylene membrane (Polycap 36 HD, Whatman, Inc., Florham Park, NJ) immediately upon arrival at the laboratory. Aliquots of the filtered samples samples were analyzed for water chemistry parameters at TestAmerica, Phoenix, AZ. The water chemistry tests were run within two weeks of the transformation studies. Total organic carbon was determined by Method SM5310 B [Standard Methods For The Examination of Water and Wastewater; American Public Health Association (APHA)]; metals were determined by Method

6010 [U.S. Environmental Protection Agency (EPA)]; anions were determined by EPA Method 300.0; suspended solids were determined by APHA Method SM2540 D.

Transformation study procedures

Water samples were allowed to reach room temperature (23-25 °C). 20 mL of each sample was transferred to a 50-mL polypropylene centrifuge tube. An appropriate volume of silver nanosphere suspension was pipetted into the sample to achieve a final particle concentration of either $2.5x10^7$ mL^{-1} or $2.5x10^5$ mL^{-1}. Each spiked sample was inverted several times, and an appropriate volume was immediately taken and spiked into reagent water to a final concentration of $2.5x10^4$ mL^{-1} for analysis by SP-ICPMS (i.e., the 1 minute sample point). Identical volumes of each spiked sample (i.e., to achieve a $2.5x10^4$ mL^{-1} analysis concentration) were taken at 12.5, 25, 50, 1400, and for some samples 2900 minutes, diluted to $2.5x10^4$ mL^{-1}, and analyzed by SP-ICPMS. Initial test sample preparations were staggered so all water samples at a given testing condition (nanomaterials and concentration) were analyzed together. Because the primary focus of the studies was to examine transformations at the more environmentally relevant low particle concentration, and transformations at high particle concentration were expected to be predominantly ionic strength related, freshwater samples were not studied at high particle concentration.

SP-ICPMS analysis

SP-ICPMS analyses were performed on a NexION 300Q (PerkinElmer, Waltham, MA). The ICPMS was tuned with multi-element tuning solution for maximum overall sensitivity and oxide and doubly charged levels conforming to manufacturer's specifications. The dwell time for all SP-ICPMS analyses was 1 ms. Each analysis consisted of a time-resolved analysis of 25,000 dwell periods, the maximum allowed by the instrument. The settling time between dwell periods was changed in the instrument registry from 100 μs to 50 μs. Shorter settling times improve the accuracy of particle element mass distributions by minimizing the loss of part of some ion plumes during the settling time (Heithmar 2009).

Calculations

The particle element mass distribution was characterized by the number-based mean particle element mass (equation 1), the mass-based mean particle element mass (equation 2), and the polydispersity index (PDI) of particle element mass (equation 3).

$$M_{mean,n} = \Sigma M_i / n \qquad \text{(equation 1)}$$

$M_{mean,m} = \Sigma M_i^2 / \Sigma M_i$ (equation 2)

$PDI_m = M_{mean,m} / M_{mean,n}$ (equation 3)

Here, M_i is the mass of the ith particle, and the summations are over all n particles detected.

The polydispersity index is a measure of the width of the particle element mass distribution. $PDI_m = 1$ for a perfectly monodisperse dispersion with respect to particle element mass. The polydispersity increases as the width of the particle element mass distribution broadens.

In addition to the determination of nanoparticle silver mass, an operational definition of "dissolved" silver was applied to the sum of the ion counts in dwell periods containing four or fewer ions, and the total silver mass in the sample was determined from the sum of the ion counts in all dwell periods of the analysis. The "dissolved" silver value was interpreted as the silver mass consistent with free silver ion. It should be noted that "dissolved" silver is an operational definition. It can be produced by free ionic silver. However, silver-containing particles that generate only a few ions and therefore cannot be distinguished from the dissolved background are also included in the "dissolved" silver mass.

Results and Discussion

Sample water chemistry

The salinity value of the open-bay Station 31 was much higher than that of the isolated bay-arm Station 7, as expected (Table 4). Also consistent with significant sea-water content, the major anion and cation concentrations in Station 31 water were much higher than any of the other three water samples. Total organic carbon and suspended solids were comparable for the two estuary samples, and much lower for the fresh water samples. Most of the organic material that colored the fresh water samples was apparently particulate matter that was retained by the 20-µm filter. In fact, there was little color in any of the four filtered samples.

Table 4. Measured water chemistry parameters for water samples used in transformation studies.

Chemistry parameter	S.F. Bay Station 7	S.F. Bay Station 31	Lake Hancock	Alafia River
Salinity (PSU)	0.07	15.8	NA	NA
Total Organic Carbon (mg/L)	26	24	2.6	2.4
Calcium (mg/L)	11	190	17	14
Magnesium (mg/L)	6.0	490	4.5	8.2
Chloride (mg/L)	8.6	9100	27	14
Sulfate (mg/L)	9.5	1200	6.8	67
Suspended Solids (mg/L)	64	48	Not detected	Not detected

Transformation of 50-nm citrate-capped silver ENM at high particle concentration

Citrate-capped 50-nm silver ENM suspensions were spiked in the two estuary waters and deionized water at a particle concentration of $2.5x10^7$ mL^{-1}. Transformations were monitored by SP-ICPMS up to 2900 minutes exposure. The mass-based mean particle Ag mass did not change over that time for either deionized water or the low salinity Station 7 water (Figure 4). In the high salinity Station 31 water, the mean particle Ag mass increased by more than four-fold compared with the other waters after 2900 minutes of exposure. This is consistent with both theory and previous laboratory studies in saline water. Both simple Derjaguin, Landau, Verwey and Overbeek (DLVO) theory and the more detailed Sogami-ISe theory predict that increased ionic strength will increase nanoparticle aggregation, by shrinking the electrical double layer; therefore, decreasing interparticle repulsion (Saleh, Kim et al. 2008; French, Jacobson et al. 2009). Initially, average particle Ag mass increases very rapidly in the high-salinity water (i.e., >1.5-fold increase in less than one minute).

Figure 4. Mass-based mean particle mass of citrate-capped 50-nm Ag over time in deionized water and low- and high-salinity estuary waters ($2.5x10^7$ mL^{-1}).

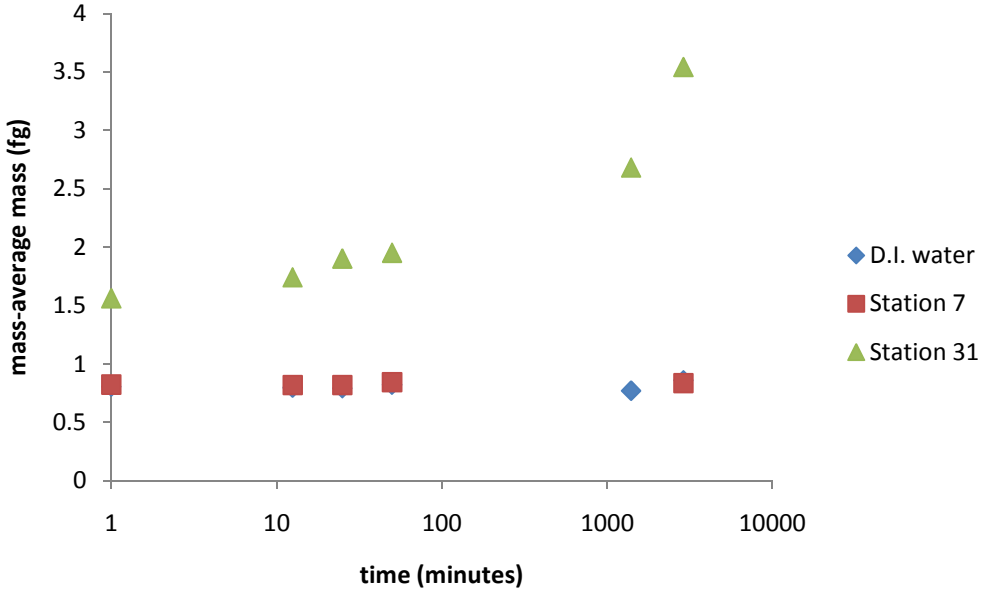

The PDI of the 50-nm Ag particle Ag mass is not affected by either Station 7 or deionized water (Figure 5). Again, there is substantial increase in the PDI of the particle Ag mass in the high salinity Station 31 water compared with the other waters, much of this increase occurring in less than 1 minute. This indicates that, in addition to shifting to higher average particle Ag mass, the particle Ag-mass distribution is broadened in Station 31 water.

Figure 5. Polydispersity index of citrate-capped 50-nm Ag over time in deionized water and low- and high-salinity estuary waters ($2.5x10^7$ mL^{-1}).

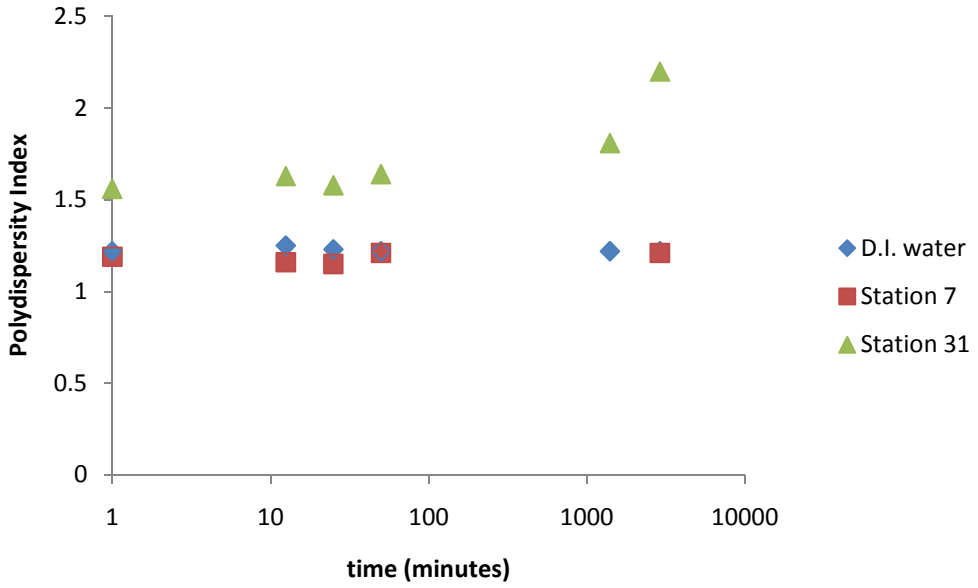

There is significant increase over time in the measured "dissolved" Ag in all three waters (Figure 6). This relative increase is 24% for deionized water, 45% for Station 7 water, and 60% for Station 31 water. As discussed previously, SP-ICPMS cannot distinguish between dissolved silver and very small silver particles. Partial dissolution of silver nanoparticles might be explained by the dilution of the excess capping agent when the standards are spiked into water.

The total mass of silver measured decreased over time for all three waters (Figure 7). The reason for this loss of silver is not fully explained at present. Some loss in total silver could be expected for the Station 31 water from precipitation of larger aggregates, but there was no observable aggregation in the other waters. One possible cause is a slow precipitation, or adsorption on the container walls, of primary particles.

Figure 6. Change in measured "dissolved" silver over time in suspensions of citrate-capped 50-nm Ag in deionized water and low- and high-salinity estuary waters ($2.5x10^7$ mL^{-1}).

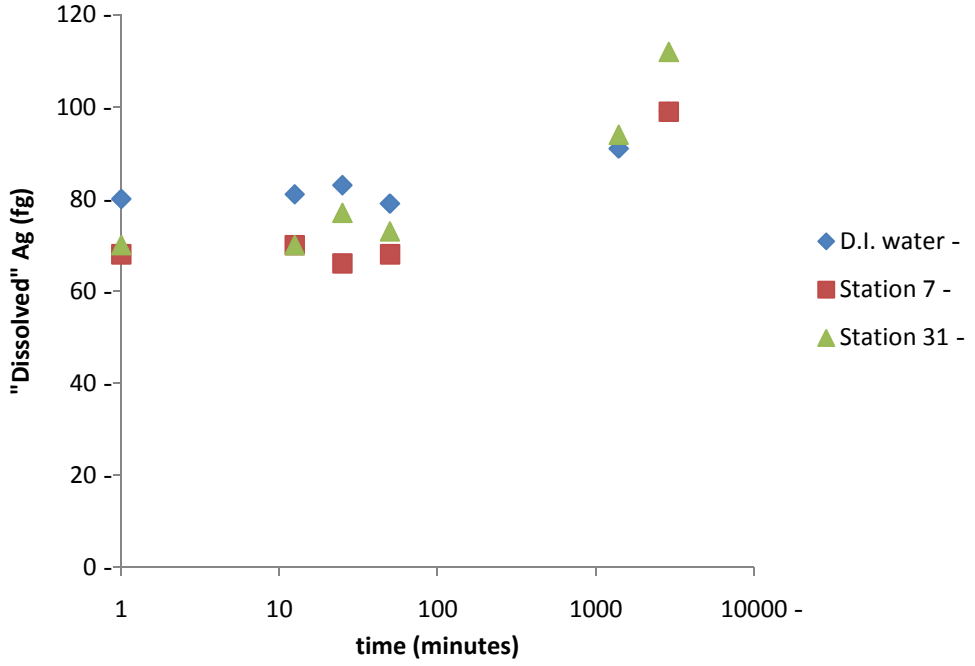

Figure 7. Change in total measured silver over time in suspensions of citrate-capped 50-nm Ag in deionized water and low- and high-salinity estuary waters ($2.5x10^7$ mL^{-1}).

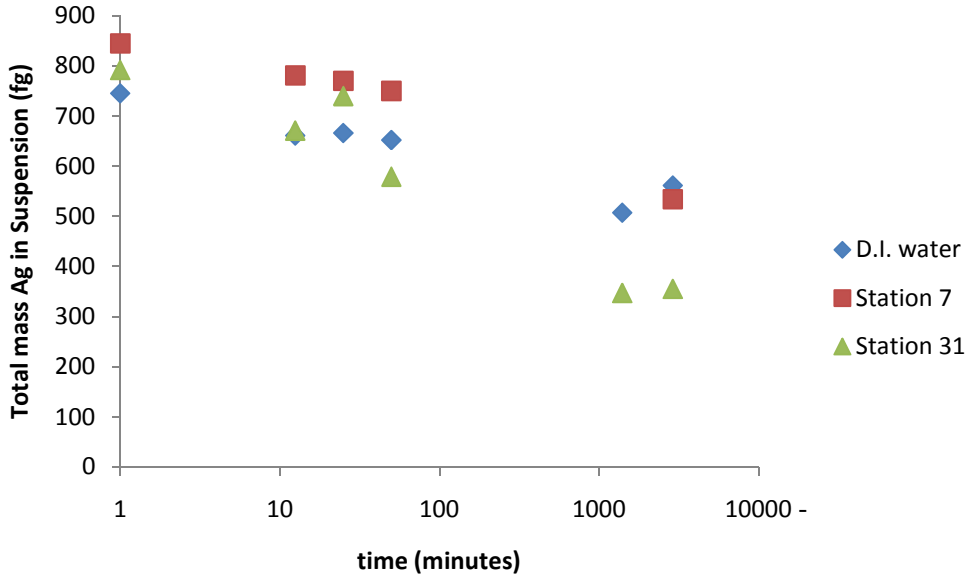

Comparison of transformations of 50-nm and 100-nm citrate-capped silver ENM

The transformation rates of 50-nm and 100-nm citrate-capped silver ENM were compared at particle concentrations of 2.5×10^7 mL^{-1} over 1400 minutes. Because transformation rates for 50-nm silver were fastest in the high-salinity Station 31 water, that sample was used for the comparison. The PDI of the particle Ag mass was used as a measure of particle aggregation. The PDI of the 50-nm silver suspension increased 16% over 1400 minutes (Figure 8). The PDI of the 100-nm suspension increased by 36% over the same time. This supports a conclusion that the rate of aggregation of silver nanoparticles increases with particle size. He et al. studied the effect of particle size on hematite nanoparticle aggregation and concluded that "at the same ionic strength, aggregation rates are higher for smaller particles (He, Wan et al. 2008). However, that study was done at constant hematite mass concentration, so it is not necessarily contradictory to the conclusion of this study. The silver mass concentration was 8 times higher in the 100-nm silver suspension than in the 50-nm suspension at the same 2.5×10^7 mL^{-1} particle concentration.

The increase in the "dissolved" silver concentration in the 100-nm silver suspension was 3.4 times the increase in the 50-nm suspension (Figure 9). Because the dissolution rate should be proportional to surface area, this is in fair agreement with the 4-fold greater surface total silver area in the former suspension.

Figure 8. Increase in PDI over time for suspensions of 50-nm and 100-nm citrate-capped Ag in high-salinity estuary water ($2.5x10^7$ mL^{-1}).

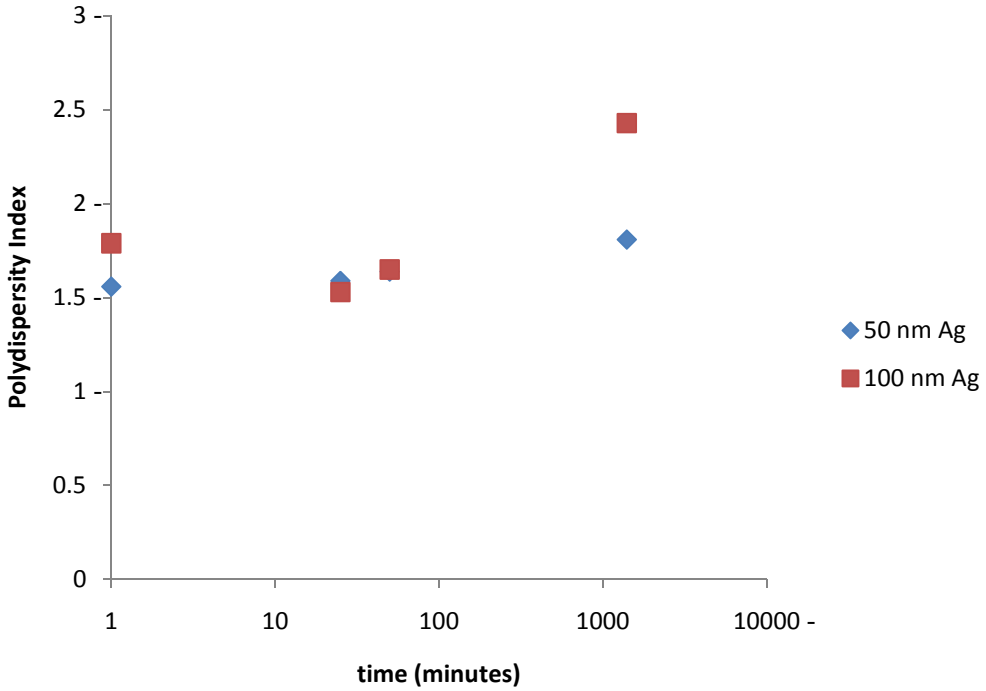

Figure 9. Increase in "dissolved" silver over time for suspensions of 50-nm and 100-nm citrate-capped Ag in high-salinity estuary water ($2.5x10^7$ mL^{-1}).

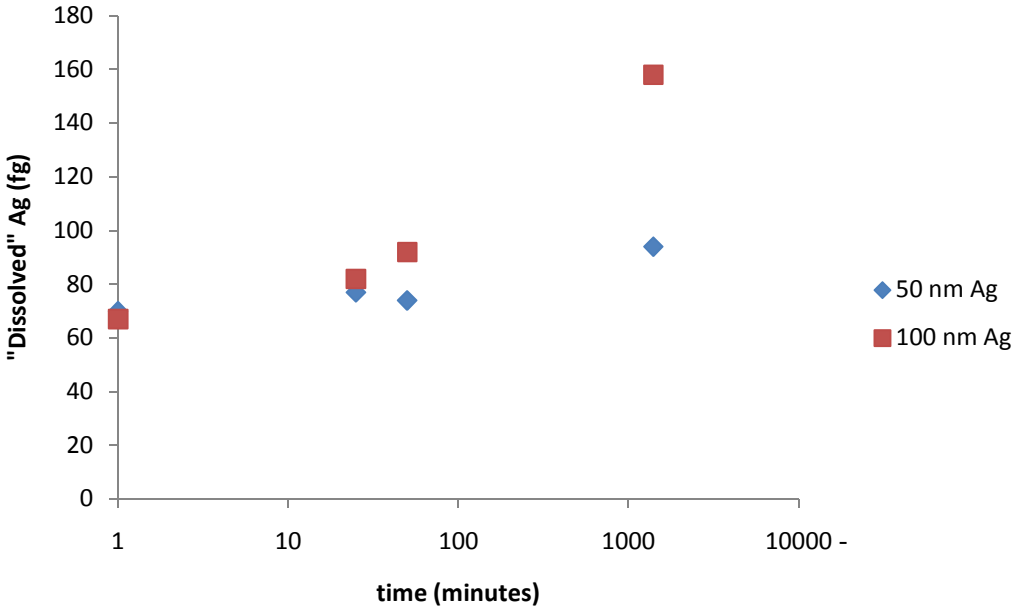

Comparison of transformations of PVP-capped and citrate-capped 50-nm silver ENM

The transformation rates of PVP-capped and citrate-capped 50-nm silver ENM were compared at particle concentrations of $2.5x10^7$ mL^{-1} over 1400 minutes. As with the previous comparison of different size particles, the high-salinity Station 31 water was used for the comparison, and the PDI of the particle Ag mass was used as a measure of particle aggregation. The PDI increase over 1400 minutes was 45% for the PVP-capped silver compared with 16% for the citrate capped silver (Figure 10).

Figure 10. Increase in PDI over time for suspensions of PVP-capped and citrate-capped 50-nm Ag in high-salinity estuary water ($2.5x10^7$ mL^{-1}).

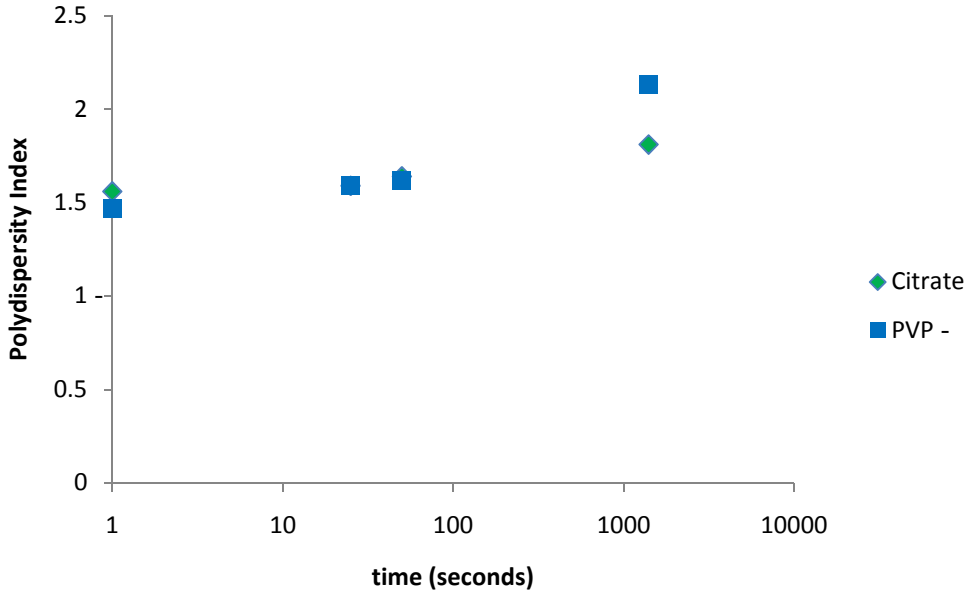

The increase in the "dissolved" silver concentration in the PVP-capped suspension over 1400 minutes is 2.25 times greater than that in the citrate-capped suspension (Figure 11), although the PVP surface area is only 18% larger.

Figure 11. Increase in "dissolved" silver over time for suspensions of PVP-capped and citrate-capped 50-nm Ag in high-salinity estuary water ($2.5x10^7$ mL^{-1}).

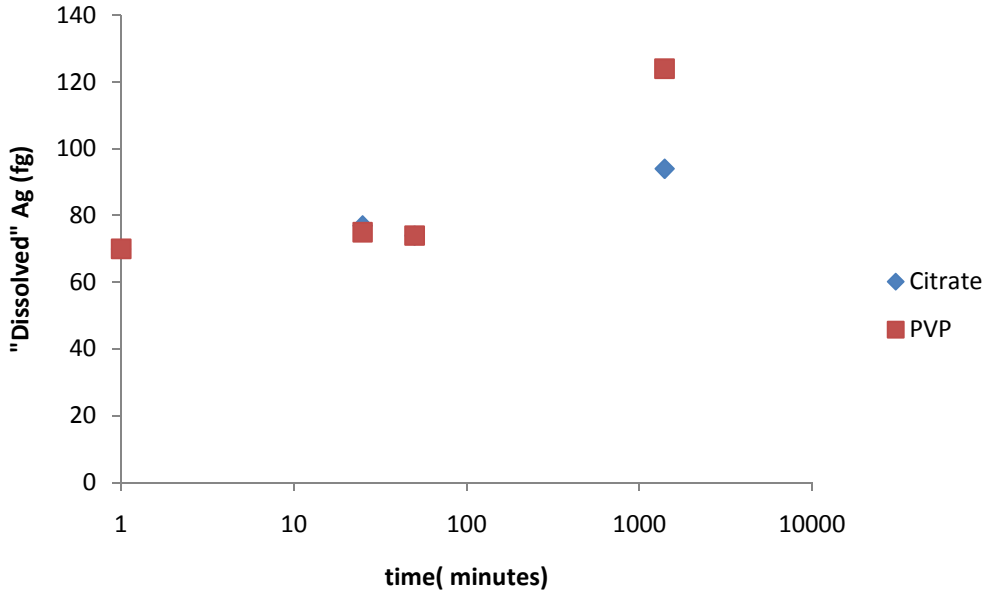

Transformation of 50-nm citrate-capped silver ENM at low particle concentration

The transformations of 50-nm citrate capped silver ENM suspensions in all four surface waters were monitored over 1400 minutes, this time at a concentration of $2.5x10^5$ mL^{-1}, 100-fold more dilute than the previous experiments. The percent changes in mass-based mean particle Ag mass, PDI of the particle Ag, measured "dissolved" Ag mass, and measured total Ag mass were calculated for 1400 minutes exposure (Figure 12). At this concentration, there is very little evidence of aggregation, in terms of either average particle Ag mass or PDI of the particle Ag mass. The single exception is a moderate increase in average particle Ag mass in the Alafia River water. These results are consistent with aggregation following pseudo second-order kinetics. There is evidence of some total silver mass loss. By far the most dominant process at this low concentration is an increase in "dissolved" silver.

Figure 12. Changes in suspension metrics of 50-nm citrate-capped silver after 1400 minutes ($2.5x10^5$ mL^{-1})

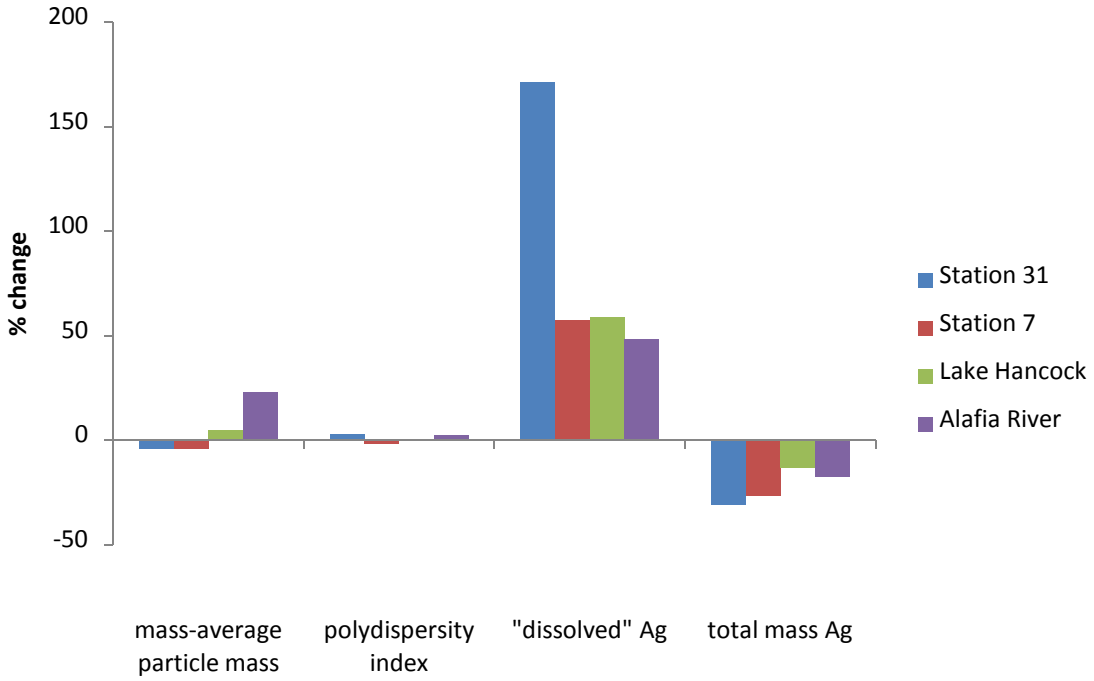

The overall % changes over 1400 minutes for $2.5x10^5$ mL^{-1} (Figure 13 – blue bars) and $2.5x10^7$ mL^{-1} (Figure 13 – red bars) were compared. Not only was apparent dissolution the dominant process at the lower concentration, the degree of apparent dissolution was more than 5-fold greater over 1400 minutes than at high concentration as a percentage of the original value. The silver mass concentration of the suspension at a particle concentration of $2.5x10^5$ mL^{-1} was 0.16 µg/L (as calculated from 20 mg/L concentration of the purchased standard). This concentration is much more realistic than the 16 µg/L concentration at a particle concentration of $2.5x10^7$ mL^{-1} with respect to the concentrations of engineered nanoparticles likely to be currently encountered in the environment.

Figure 13. Effect of concentration on changes in suspension metrics of 50-nm citrate-capped silver after 1400 minutes ($2.5x10^5$ mL^{-1})

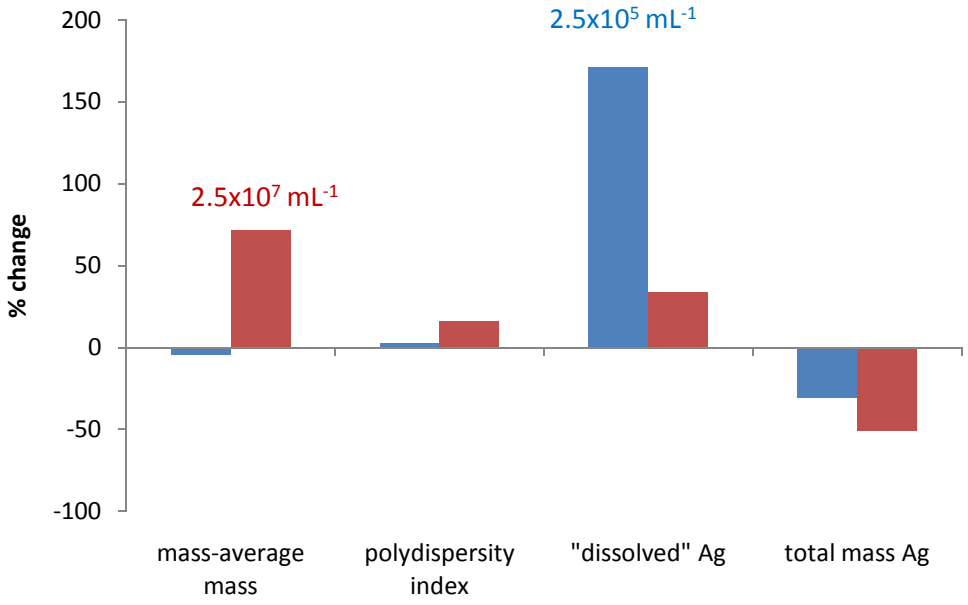

Conclusions and Future Work

The study reported here demonstrates the effectiveness of SP-ICPMS for rapidly screening surface water for metal-containing nanoparticles. This capability would allow large numbers of water samples to be screened. The samples showing possible presence of target nanoparticles could then be analyzed by more selective techniques that are much more time-consuming and costly. The study reported here shows another advantage of the rapid screening capability of SP-ICPMS. Rates of transformations, such as aggregation and dissolution, can be studied with high temporal resolution. In this case, the data related to aggregation is reliable even in complex water matrices. Dissolution information is screening-level, because SP-ICPMS cannot differentiate dissolved metal from very small nanoparticles. The sensitivity of current ICPMS instruments precludes SP-ICPMS from distinguishing particles smaller than about 15-20 nm from dissolved silver. This would prohibit its use in studying primary particles of consumer products containing small nanoparticles. On the other hand, SP-ICPMS could also be used to study disaggregation if the primary particles are larger than this lower limit.

This study confirms the results of other studies of aggregation of nanoparticles at high ionic strength and high ($>10^7$ mL^{-1}) nanoparticle concentrations in both synthetic laboratory media (Saleh, Kim et al. 2008; French, Jacobson et al. 2009; Trinh, Kjøniksen et al. 2009) and natural water (Chinnapongse, MacCuspie et al. 2011). Those studies all found that aggregation of a variety of nanoparticles increased with increasing ionic strength. However, this study also shows that at low silver nanoparticle concentration ($2.5x10^5$ mL^{-1}), aggregation is minimal over 24 hours, even in highly saline estuary water. Instead, the dominant process is one that is consistent with either dissolution of the nanoparticles or formation of smaller nanoparticles that cannot be experimentally distinguished from dissolved. This has not been observed in previous studies because the sensitivity of the analytical techniques used could not study transformation at low nanoparticle concentration. Studies in this concentration regime are critical, because it is the range of expected environmental concentrations of engineered nanoparticles (Kiser, Westerhoff et al. 2009).

These transformation study results are preliminary and more detailed research is planned. These additional studies will investigate the role of natural organic matter on transformations at low nanoparticle concentration, to compare with previous studies at high concentration that found suppression of aggregation by NOM (Liu, Wazne et al. 2010; Thio, Zhou et al. 2011). The effects of pH, temperature, and oxygen saturation should also be investigated. Finally, ultrafiltration and other approaches will be explored to elucidate the nature of the "dissolved" silver. Finally, hyphenated methods will be developed.

References

Alvarez, P. J. J., V. Colvin, et al. (2009). "Research Priorities to Advance Eco-Responsible Nanotechnology." ACS Nano **3**(7): 1616-1619.

Chinnapongse, S. L., R. I. MacCuspie, et al. (2011). "Persistence of singly dispersed silver nanoparticles in natural freshwaters, synthetic seawater, and simulated estuarine waters." Science of The Total Environment **409**(12): 2443-2450.

Degueldre, C. and P. Y. Favarger (2004). "Thorium colloid analysis by single particle inductively coupled plasma-mass spectrometry." Talanta **62**(5): 1051-1054.

Degueldre, C., P. Y. Favarger, et al. (2004). "Zirconia colloid analysis by single particle inductively coupled plasma-mass spectrometry." Analytica Chimica Acta **518**(1-2): 137-142.

Degueldre, C., P. Y. Favarger, et al. (2006). "Gold colloid analysis by inductively coupled plasma-mass spectrometry in a single particle mode." Analytica Chimica Acta **555**(2): 263-268.

Ebenstein, Y., E. Nahum, et al. (2002). "Tapping Mode Atomic Force Microscopy for Nanoparticle Sizing: Tipâˆ'Sample Interaction Effects." Nano Letters **2**(9): 945-950.

Filella, M., J. Zhang, et al. (1997). "Analytical applications of photon correlation spectroscopy for size distribution measurements of natural colloidal suspensions: capabilities and limitations." Colloids and Surfaces A: Physicochemical and Engineering Aspects **120**(1-3): 27-46.

French, R. A., A. R. Jacobson, et al. (2009). "Influence of Ionic Strength, pH, and Cation Valence on Aggregation Kinetics of Titanium Dioxide Nanoparticles." Environmental Science & Technology **43**(5): 1354-1359.

Gray, P. J., J. W. Olesik, et al. (2009). Particle Size Effects on Vaporization in Laser Ablation Inductively Coupled Plasma Mass Spectrometry. Pittsburgh Conference on Analytical Chemistry and Applied Spectroscopy, Chicago, IL.

Handy, R., F. von der Kammer, et al. (2008). "The ecotoxicology and chemistry of manufactured nanoparticles." Ecotoxicology **17**(4): 287-314.

Hassellöv, M. (2009). Detection and Characterization of engineered nanoparticle in the enviroment using Field-Flow Fractionation coupled to ICP-MS in single nanoparticle detection mode. Goteborg Setac Europe.

Hassellöv, M., J. Readman, et al. (2008). "Nanoparticle analysis and characterization methodologies in environmental risk assessment of engineered nanoparticles." Ecotoxicology **17**(5): 344-361.

He, Y., J. Wan, et al. (2008). "Kinetic stability of hematite nanoparticles: the effect of particle sizes." Journal of Nanoparticle Research **10**(2): 321-332.

Heithmar, E. (2009). Characterizing Metal-based Nanoparticles in Surface Water by Single-Particle ICPMS. 237th ACS National Meeting, Salt Lake City, Utah.

Kammer, F. v. d., M. Baborowski, et al. (2005). "Field-flow fractionation coupled to multi-angle laser light scattering detectors: Applicability and analytical benefits for the analysis of environmental colloids." Analytica Chimica Acta **552**(1-2): 166-174.

Kim, T., C.-H. Lee, et al. (2008). "Kinetics of gold nanoparticle aggregation: Experiments and modeling." Journal of Colloid and Interface Science **318**(2): 238-243.

Kiser, M. A., P. Westerhoff, et al. (2009). "Titanium Nanomaterial Removal and Release from Wastewater Treatment Plants." Environmental Science & Technology **43**(17): 6757-6763.

Klaine, S. J., P. J. J. Alvarez, et al. (2008). "NANOMATERIALS IN THE ENVIRONMENT: BEHAVIOR, FATE, BIOAVAILABILITY, AND EFFECTS." Environmental Toxicology & Chemistry **27**: 1825-1851.

Koirtyohann, S. R., J. S. Jones, et al. (1980). "Nomenclature system for the low-power argon inductively coupled plasma." Analytical Chemistry **52**(12): 1965-1966.

Lam, J. W. H. and G. Horlick (1990). "A Comparison of Argon and Mixed Gas Plasmas for Inductively Coupled Plasma-mass Spectrometry." Spectrochimica Acta Part B: Atomic Spectroscopy **45**.

Lesher, E. K., J. F. Ranville, et al. (2009). "Analysis of pH Dependent Uranium(VI) Sorption to Nanoparticulate Hematite by Flow Field-Flow Fractionation - Inductively Coupled Plasma Mass Spectrometry." Environmental Science & Technology **43**(14): 5403-5409.

Lin, W.-C. and M.-C. Yang (2005). "Novel Silver/Poly(vinyl alcohol) Nanocomposites for Surface-Enhanced Raman Scattering-Active Substrates." Macromolecular Rapid Communications **26**(24): 1942-1947.

Liu, X., M. Wazne, et al. (2010). "Effects of natural organic matter on aggregation kinetics of boron nanoparticles in monovalent and divalent electrolytes." Journal of Colloid and Interface Science **348**(1): 101-107.

Monserud, J. H., E. K. Lesher, et al. (2009). Real Time Single Particle-inductively Coupled Plamsa-mass Spectrometry for Detection and Characterization of Nanoparticles. 237th ACS National Meeting, Salt Lake City, Utah.

Mueller, N. C. and B. Nowack (2008). "Exposure Modeling of Engineered Nanoparticles in the Environment." Environmental Science & Technology **42**: 4447-4453.

O'Connor, G. and E. H. Evans (1999). Fundamental aspects of ICP-MS. Inductively Coupled Plasma Spectrometry and its Applications. S. J. Hill. Sheffield, Sheffield Academic Press**:** 119-144.

Pyrz, W. D. and D. J. Buttrey (2008). "Particle Size Determination Using TEM: A Discussion of Image Acquisition and Analysis for the Novice Microscopist." Langmuir **24**(20): 11350-11360.

Saleh, N., H.-J. Kim, et al. (2008). "Ionic Strength and Composition Affect the Mobility of Surface-Modified Fe0 Nanoparticles in Water-Saturated Sand Columns." Environmental Science & Technology **42**(9): 3349-3355.

Schulte, P., C. Geraci, et al. (2008). "Occupational Risk Management of Engineered Nanoparticles." Journal of Occupational & Environmental Hygiene **5**: 239-249.

Schurtenberger, P., M. E. Newmen, et al. (1993). "Environmental Particles." J. Buffle, H.P. van Leeuwen (Eds) **2**: 37.

Takagi, A., A. Hirose, et al. (2008). "Induction of mesathelioma in p53+/- mouse by intraperitioneal application of multi-wall carbon nanotube." Journal of Toxicol Science **33**: 105-116.

Tang, Z., L. Wu, et al. (2009). "Size fractionation and characterization of nanocolloidal particles in soils." Environmental Geochemistry and Health **31**(1): 1-10.

Taylor, H. E. (2001). Inductively Coupled Plasma-Mass Spectrometry: Practices and Techniques. San Diego, Academic Press.

Thio, B. J. R., D. Zhou, et al. (2011). "Influence of natural organic matter on the aggregation and deposition of titanium dioxide nanoparticles." Journal of Hazardous Materials **189**(1-2): 556-563.

Thomas, R. (2004). Practical Guide to ICP-MS. New York, Marcel Dekker, Inc.

Tiede, K., A. B. A. Boxall, et al. (2010). "Application of hydrodynamic chromatography-ICP-MS to investigate the fate of silver nanoparticles in activated sludge." Journal of Analytical Atomic Spectrometry **25**(7): 1149-1154.

Tiede, K., M. Hassellöv, et al. (2009). "Considerations for environmental fate and ecotoxicity testing to support environmental risk assessments for engineered nanoparticles." Journal of Chromatography A **1216**(3): 503-509.

Trinh, L., A.-L. Kjøniksen, et al. (2009). "Slow salt-induced aggregation of citrate-covered silver particles in aqueous solutions of cellulose derivatives." Colloid & Polymer Science **287**(12): 1391-1404.

United States
Environmental Protection
Agency

Office of Research
and Development (8101R)
Washington, DC 20460

Official Business
Penalty for Private Use
$300

EPA/600/R-11/096
September 2011
www.epa.gov

Please make all necessary changes on the below label, detach or copy and return to the address in the upper left hand corner.

If you do not wish to receive these reports CHECK HERE ☐; detach, or copy this cover, and return to the address in the upper left hand corner.

PRESORTED STANDARD
POSTAGE & FEES PAID
EPA PERMIT No. G-35